第 54 卷第 4 期
2026 年 4 月

硅 酸 盐 学 报
JOURNAL OF THE CHINESE CERAMIC SOCIETY

Vol. 54，No. 4
April，2026

http://jccsoc.cbpt.cnki.net

DOI：10.14062/j.issn.0454-5648.20250430

化学计量碱金属二硅酸盐玻璃–晶体界面能的分子动力学研究：基于晶体最小能量切割法

LETON Chandra Saha, TETSUYA Murata, SHINGO Nakane

(日本电气硝子株式会社基础技术事业部，滋贺县大津市 520-8639，日本)

摘　要：为估算玻璃与晶体之间的界面能(σ)，基于 Tielemann 理论，采用分子动力学模拟开发了一种晶体最小能量切割界面模型。使用该模型可复现实验测得的化学计量碱金属二硅酸盐(如 $Li_2O{\cdot}2SiO_2$、$Na_2O{\cdot}2SiO_2$ 与 $K_2O{\cdot}2SiO_2$)玻璃–晶体体系中界面能规律，即 $\sigma_{Li} > \sigma_{Na} > \sigma_K$。进一步通过分析界面配位数($CN_{int}$)，推导出键强–配位数关系，该关系与界面能存在内在关联。

关键词：玻璃–晶体界面能；分子动力学模拟；原子间势函数；界面配位数
中图分类号：TQ175　　**文献标志码**：A　　**文章编号**：0454–5648(2026)04–1291–08
网络出版时间：2025–11–10

1 Introduction

Crystallization control is crucial during glass production[1–3]. In glass crystallization theory[4], it has been hypothesized that there is a direct relationship between glass-crystal interfacial energy and nucleation rate[5]. Since it is difficult to measure interfacial energy directly, classical nucleation theory is used to obtain it[6]. However, the estimation process is complex; Various measurement data such as the nucleation rate, viscosity, and Gibbs free energy barriers between the glass and crystal are required. Overall, estimating the glass-crystal interfacial energy is time-consuming. In this regard, the interfacial energy can be directly obtained using molecular dynamics (MD) simulations, as reported in various studies[3, 7].

The calculation of interfacial energy between a TiO_2 crystal and sodium silicate glass[7] and the stoichiometric/non-stoichiometric glass-crystal interfaces for anorthite using MD have been reported[3]. Moreover, the effects of the surface orientation and termination plane on the glass–crystal interface of lithium disilicates have also been studied[8]. In previous MD studies on glass-crystal interfaces[3,7–8], crystal orientation planes were constructed by single cuts through the crystal structure, which may not be the representative optimal positions. Therefore, a suitable method is required to obtain crystal orientation planes for constructing an interfacial model.

In this study, we implemented an interface model to estimate the glass-crystal interfacial energy based on the theory of Tielemann *et al.*[5], which was recently introduced to generate crystal orientation planes using minimum-energy cuts. To the best of our knowledge, this is the first work in which the crystal orientation plane determined based on a minimum-energy cutting process has been used to build a glass-crystal interface in a more realistic environment (*i.e.*, hypothesizes that a minimum-energy structure may occur during crystal nucleation) and calculate the interfacial energy. To achieve this, we considered stoichiometric alkali (Li, Na, and K) disilicate ($2SiO_2$) glasses and crystals, as some early-stage experimental data have been reported[9], which are highly beneficial for validating the MD results.

The effects of different potential models were also investigated and found that they had a significant impact on the reproduction of the experimental trend. In addition, we performed analyses of some structural aspects, such as the coordination number distribution of cations with neighboring anions across the glass-crystal interface, and the cation–anion bond strength-coordination number.

2 Computational details

2.1 Interfacial models

Stoichiometric glass and crystal structures were used to create the interfacial models, namely Li_2O-$2SiO_2$, Na_2O-$2SiO_2$, and K_2O-$2SiO_2$. A schematic interfacial

收稿日期：2025–06–03。　修订日期：2025–07–18。
第一作者：LETON Chandra Saha (1980—)，男，博士，主任研究员。

Received date: 2025–06–03.　**Revised date:** 2025–07–18.
First author: LETON Chandra Saha (1980–), male, Ph.D, Senior researcher.
E-mail: lsaha@neg.co.jp

model is presented in Fig. 1, where γ_{hkl} represents the crystal plane energy through the minimum energy cut in the crystal structure. More details regarding the minimum-energy cutting process are described in the Ref.[5].

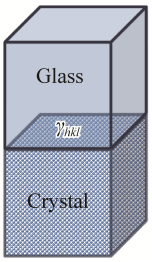

Fig. 1 Illustration of the interfacial model between glass and crystal, where the glass is on top of the crystal. γ_{hkl} is an indicator to find the energy of the crystal plane

It has been reported that the low-index lattice planes (*hkl*) are dominated by (100), (010), and (001) [5,10]. Therefore, the three crystal planes (001), (010), and (001) were considered for each crystal structure of Li_2O-$2SiO_2$, Na_2O-$2SiO_2$, and K_2O-$2SiO_2$, respectively, to form interfaces with the glass structure. The crystal structures of Li_2O-$2SiO_2$, Na_2O-$2SiO_2$, and K_2O-$2SiO_2$ can be found elsewhere, respectively[11–13]. The interfacial model was constructed using the lowest value of γ_{hkl} among the three low-index lattice planes. The value of γ_{hkl} was estimated as follows:

$$\gamma_{hkl} = \frac{1}{N_A}\sum_i \frac{S_{i,hkl}}{A_{hkl}} U_i \quad (1)$$

where S_i is the number of cation-anion bonds broken, and N_A denotes Avogadro's constant. A_{hkl} is the area of the *hkl* plane. U_i refers to the cation (Si, Li, Na, and K)–anion (O) bond energy, which was collected from Ref.[5]. Table 1 shows the lowest calculated value of γ_{hkl} for the different crystal structures. The three models based on the value of γ_{hkl} are Li_2O-$2SiO_2$ glass–Li_2O-$2SiO_2$ (001), Na_2O-$2SiO_2$ glass–Na_2O-$2SiO_2$ (010), and $K_2O{\cdot}2SiO_2$ glass–K_2O-$2SiO_2$ (001).

Table 1 Lowest values of γ_{hkl} for Li_2O-$2SiO_2$, Na_2O-$2SiO_2$, and K_2O-$2SiO_2$

Crystal	(*hkl*)	γ_{hkl}/(J·m^{-2})
Li_2O-$2SiO_2$	(001)	1.00
Na_2O-$2SiO_2$	(010)	0.54
K_2O-$2SiO_2$	(001)	2.00

The dimensions of the Li_2O-$2SiO_2$ glass–Li_2O-$2SiO_2$ (001), Na_2O-$2SiO_2$ glass–Na_2O-$2SiO_2$ (010), and K_2O-$2SiO_2$ glass–K_2O-$2SiO_2$ (001) interfaces were (*x*) 62.51 Å ×(*y*) 62.19 Å ×(*z*) 117.18 Å; (*x*) 58.75 Å × (*y*) 57.68 Å × (*z*) 123.38 Å; and (*x*) 59.46 Å × (*y*) 55.55 Å × (*z*) 142.68 Å, respectively. The number of atoms in the glass-crystal interface models of Li_2O-$2SiO_2$, Na_2O-$2SiO_2$, and K_2O-$2SiO_2$ were 41 184, 31 104, and 31 104, respectively. The glass and crystal structures had an equal number of atoms.

The glass structure was fabricated from the crystal structures by simulating a melt-quenching process. First, the Li_2O-$2SiO_2$ (001), Na_2O-$2SiO_2$ (010), and K_2O-$2SiO_2$ (001) crystal structures were prepared. Half the crystal was kept fixed, while the other half was melted at 3500 K with a canonical ensemble (NVT) for 300 ps and then quenched to 300 K at a cooling rate of 5 K/ps. After the melt-quenching process, the crystal part was unfixed and relaxed for 200 ps with a glassy structure using an isobaric–isothermal ensemble (NPT) at a temperature of 300 K.

2.2 Potential models

We used three interatomic potential models to estimate the interfacial energies of Li_2O-$2SiO_2$ glass–Li_2O-$2SiO_2$ (001), Na_2O-$2SiO_2$ glass–Na_2O-$2SiO_2$ (010), and K_2O-$2SiO_2$ glass–K_2O-$2SiO_2$ (001). All three of these potential functions are widely used, and each is briefly described below.

2.2.1 Pedone potential To simulate silica-based glasses, Pedone *et al*. [14] derived a set of interatomic pairwise potential parameters using results from crystalline structures. The potential function proposed by Pedone *et al*. is as follows:

$$V(r_{ij}) = \frac{1}{4\pi\varepsilon_0}\frac{q_i q_j}{r_{ij}} + D_{ij}\left[\left\{1-\mathrm{e}^{-a_{ij}(r-r_0)}\right\}^2 - 1\right] + \frac{C_{ij}}{r_{ij}^{12}} \quad (2)$$

Where the first term is the Coulomb interaction, the second term refers to the Morse function, and the third term indicates the repulsive contribution. The parameters D_{ij}, r_0, a_{ij} and C_{ij} are provided in Ref.[14]. The parameter of C_{ij} is related to the repulsive contribution. The long-range effects of Coulomb interactions were calculated by the particle-particle particle-mesh (PPPM) solver with a convergence criterion of 10^{-5}.

2.2.2 Du potential To study multicomponent oxide glasses, Du *et al.* [15] developed a set of potential parameters using results from crystalline structures. The potential function proposed by Du *et al*. is given by:

$$V(r_{ij}) = \frac{1}{4\pi\varepsilon_0}\frac{q_i q_j}{r_{ij}} + A_{ij}\mathrm{e}^{\frac{-r}{\rho_{ij}}} - \frac{C_{ij}}{r_{ij}^6}, \quad r_{ij} > r_0 \quad (3)$$

$$V(r_{ij}) = B_{ij}/r_{ij}^n + D_{ij}\cdot r_{ij}^2, \quad r_{ij} < r_0 \quad (4)$$

The adopted potential form is a combination of Coulombic and Buckingham terms. The parameters A_{ij}, ρ_{ij}, and C_{ij} can be found elsewhere[15]. The parameters B_{ij}, n, and D_{ij} are necessary to avoid attraction at small distances. The parameter r_0 is the transition point between the Buckingham and repulsion parts. The long-range effects of Coulomb interactions were similar to those of the Pedone potential.

2.2.3 SHIK potential Sundararaman developed the SHIK potential for oxide glasses[16]. In this case, the interatomic potential model was developed using results from the ab initio MD calculations of oxide melts. The

potential function of Sundararaman *et al.* [16] is expressed as:

$$V(r_{ij}) = A_{ij}\mathrm{e}\left(-B_{ij}r_{ij}\right) - \frac{C_{ij}}{r_{ij}^{6}} + \frac{D_{ij}}{r_{ij}^{24}} + V^{\mathrm{w}}\left(r_{ij}\right) \quad (5)$$

$$V^{\mathrm{w}}(r_{ij}) = \left[\frac{1}{r_{ij}} - \frac{1}{r_{\mathrm{cut}}} + \frac{\left(r_{ij} - r_{\mathrm{cut}}\right)}{\left(r_{\mathrm{cut}}\right)^{2}}\right] q_i q_j \quad (6)$$

The adopted potential form is a combination of a Buckingham term and a Coulombic interaction term obtained using the Wolf truncation [17] method ($V^{\mathrm{w}}(r)$). The parameters of A_{ij}, B_{ij}, C_{ij}, and D_{ij} are collected from Ref.[16]. The parameter D_{ij} is necessary to avoid attraction at small distances.

2.3 Molecular dynamics setup

The MD simulations were performed using the LAMMPS package[18]. The temperature and pressure were controlled with the Nose–Hoover thermostat and barostat, respectively[19–21]. After setting up the glass–crystal interface using NPT (see Section 2.1), we ran MD simulations with NVT for another 200 ps to calculate the interfacial energy. The MD simulations were performed with a time step of 1 fs. Periodic boundary conditions were applied in all directions. Cutoff distances were applied according to references [14–16].

3 Results and discussion

3.1 Glass density

After setting up the interface structure between the glass and crystal, we first evaluated the glass density by calculating the local density profile along the *z*-direction of Li_2O-$2SiO_2$ glass–Li_2O-$2SiO_2$ (001), Na_2O-$2SiO_2$ glass–Na_2O-$2SiO_2$ (010), and K_2O-$2SiO_2$ glass–K_2O-$2SiO_2$ (001), as shown in Fig. 2 with snapshots of the atoms in the interfacial region. The *z*-density ($\rho(z)$) was calculated as follows:

$$\rho(z) = \frac{N_z \times m}{L_x L_y \Delta z} \quad (7)$$

where L_x and L_y indicate the box lengths along the x and y direction, respectively. Δz is a bin width along the *z*-direction, and N_z indicates the number of atoms. m refers to atomic mass.

Fig. 2a – Fig. 2c demonstrate the glass structures show density results comparable to the experimental data [10, 22–25] in the glass-crystal interface structures of Li_2O-$2SiO_2$, Na_2O-$2SiO_2$, and K_2O-$2SiO_2$. The atomic configurations of the glass-crystal interface region are presented in the inset of Fig. 2, where ordered (high-intensity $\rho(z)$) and disordered (low-intensity $\rho(z)$) atoms indicate crystalline, glassy states, respectively. Later on, we will discuss the influence of the cation (Li, Na, and K)–anion environment in the interface region of each system. Only the results for the SHIK potential model are presented in Fig. 2. The effect of the different potential models was analyzed only for the interfacial energy calculations, as described in the following section.

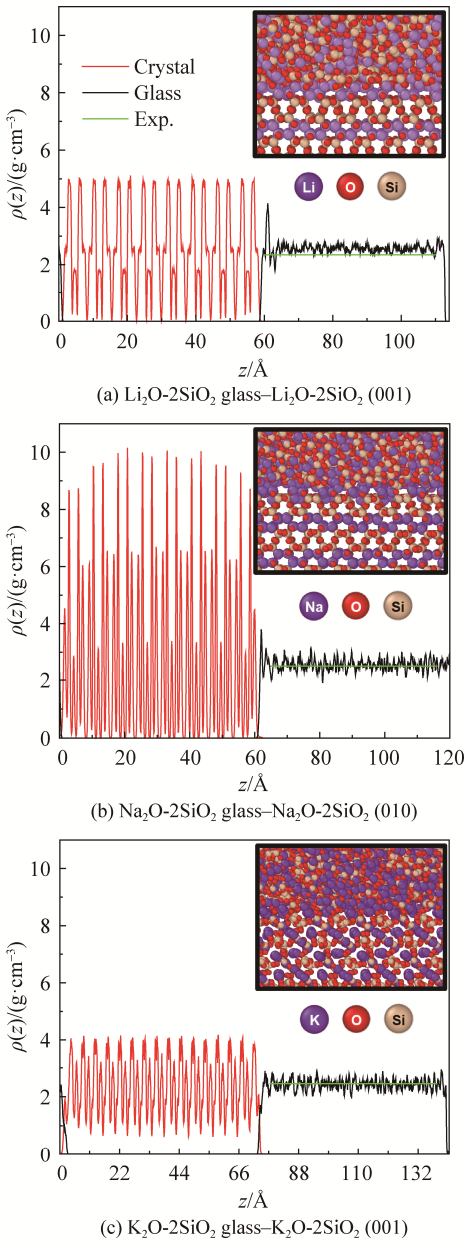

(a) Li_2O-$2SiO_2$ glass–Li_2O-$2SiO_2$ (001)

(b) Na_2O-$2SiO_2$ glass–Na_2O-$2SiO_2$ (010)

(c) K_2O-$2SiO_2$ glass–K_2O-$2SiO_2$ (001)

Fig. 2　*z*-density ($\rho(z)$) along the *z*-direction (In the inset, a side view snapshot of the atoms in the interfacial region after 200 ps, where the upper disordered atoms are glass, and the lower ordered atoms are crystalline.)

3.2 Interfacial energy and potential effect

To estimate the interfacial energy, we implemented the formulation proposed by Fossati *et al.*[7]:

$$\sigma = \frac{E_{\mathrm{glass/crystal}} - N_{\mathrm{glass}}E_{\mathrm{glass}}^{\mathrm{bulk}} - N_{\mathrm{crystal}}E_{\mathrm{crystal}}^{\mathrm{bulk}}}{2A} \quad (8)$$

where $E_{\mathrm{glass/crystal}}$ is the total energy of the interface structure (see Fig. 1) between the glass and crystal. A is the surface area of the interface. N_{glass} and N_{crystal} are the number of glass and crystal formula units, respectively. $E_{\mathrm{glass}}^{\mathrm{bulk}}$ and $E_{\mathrm{crystal}}^{\mathrm{bulk}}$ indicate the total

energies of the formula units in the bulk glass and crystal, respectively. Note that $E^{\text{bulk}}_{\text{glass}}$ and $E^{\text{bulk}}_{\text{crystal}}$ were calculated separately under the same calculation conditions as for $E_{\text{glass/crystal}}$, but to keep the crystal structure intact, we omitted the molten part for $E^{\text{bulk}}_{\text{crystal}}$.

The σ values calculated for the glass-crystal interfaces of Li_2O-$2SiO_2$, Na_2O-$2SiO_2$, and K_2O-$2SiO_2$ using the various potential models are presented along with the experimental data [9, 26] in Fig. 3.

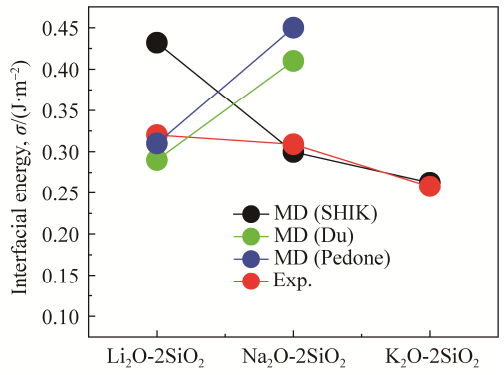

Fig. 3 Calculated σ values for the alkali disilicates using the various potential functions, along with experimental data

It should be mentioned that the experimental data were measured using a maximum-pull-on-cylinder method to obtain the surface tension of a series of lithium, sodium, and potassium silicate melts[9]. These measurement data have previously been utilized as the interfacial energy in the phase-field method for the glass-crystal interfaces of Li_2O-$2SiO_2$, Na_2O-$2SiO_2$, and K_2O-$2SiO_2$[26]. The experimental values follow the trend $\sigma_{Li}>\sigma_{Na}>\sigma_K$. The σ values calculated using the SHIK potential show a similar trend, while the Du and Pedone potentials are unable to reproduce the experimental trend. However, the potentials of Du and Pedone show better values of σ for the glass-crystal interface of Li_2O-$2SiO_2$ than the SHIK. Our MD results demonstrate that among the potential models, SHIK is a good candidate for calculating σ in terms of experimental reproduction. Note that such potential effects on glass properties have been previously reported[27], but to our knowledge, this is the first study of the glass-crystal interface of alkali disilicates.

3.3 Distribution of coordination number across the glass-crystal interfaces

We analyzed the interfacial coordination number (CN_{int}) in the contact area between the glass and crystal surfaces. These coordination numbers are difficult to estimate experimentally. Typically, the coordination number is determined in the bulk region of a glass or crystal structure. However, the coordination number across the interfacial area has previously been reported for polymer-water systems using molecular dynamics simulations[28–29], and the results showed a correlation with heat conduction. Thus, CN_{int} could have an impact on the σ value. To calculate CN_{int}, the interfacial domain must first be defined; therefore, CN_{int} was determined from the overlapping area to the minimum density (see Section 3.1) of the highest peak, as presented in Fig. 4 only for Li_2O-$2SiO_2$ glass–Li_2O-$2SiO_2$ (001).

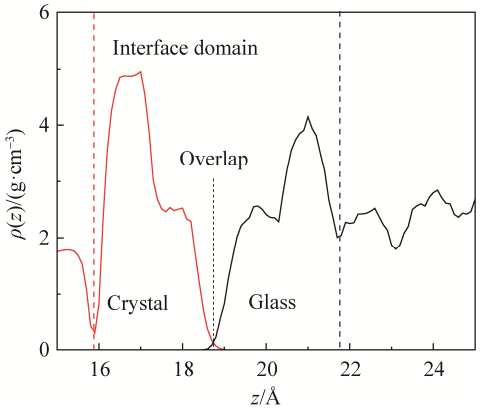

Fig. 4 z-density of the highest peak for the glass-crystal interface of Li_2O-$2SiO_2$ (The red and black dotted lines indicate the minima after the maximum peak from the overlap position, which is regarded as the interface domain.)

Next, the bond distance (r_{ij}) between the cation (Si, Li, Na, and K) and anion (O) in that domain was calculated as follows:

$$r_{ij} = \sqrt{(r_i - r_j)^2} \tag{9}$$

where r_i and r_j are the position vectors of the cation from the glass and the anion from the crystal, respectively, as shown in Fig. 5. Note that the reverse calculation was also taken into account.

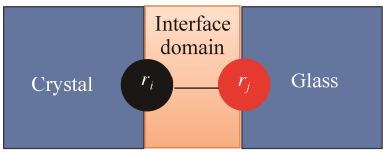

Fig. 5 Illustration of cations and anions in the glass-crystal interface region. r_i and r_j indicate the cation and anion position

Finally, CN_{int} was obtained by setting the cutoff distance (R_c) as $r_{ij}<R_c$, where R_c is the location of the first minimum after the first peak at r_{ij}. The distributions of Si—O and alkali (A = Li, Na, and K)—O as functions of r_{ij} (*i.e.*, Si—O and A—O) are presented in Fig. 6. The location of the first peak indicates the length of the Si—O and A (Li, Na, and K)—O bonds. As shown in Fig. 6 (a), the Si—O bond lengths at the glass-crystal interfaces of Li_2O-$2SiO_2$, Na_2O-$2SiO_2$, and K_2O-$2SiO_2$ were found to be similar (1.61 Å). For Li—O, Na—O, and K—O, the calculated bond lengths were 1.7, 2.2 Å, and 2.7 Å,

respectively (Fig. 6b). The calculated interfacial bonds are similar to the cation (Si and A)–anion bonds that exist in the glass or crystal structures[8, 11–13, 30–32]. However, the bond length of Li—O was found to be slightly shorter than the reported value[8, 11] in glass or crystal structures, which could be related to the potential model as we see higher σ in SHIK (see Fig. 3).

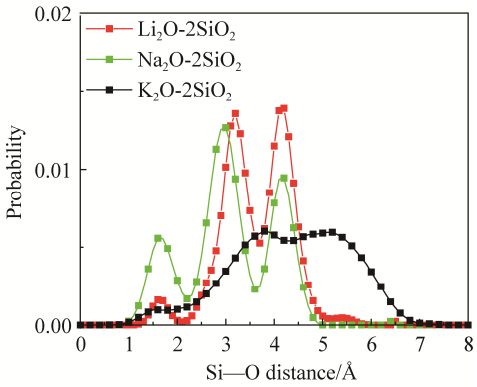

(a) Si—O

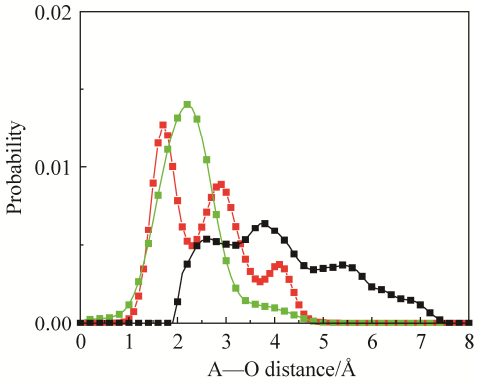

(b) Alkali (A = Li, Na, and K)—O

Fig. 6　Interfacial bond distance distribution

Fig. 7 shows the distribution of CN_{int} for the A (Li, Na, and K)—O bonds. We can see that CN_{int} varies significantly at the glass-crystal interface of Li_2O-$2SiO_2$, Na_2O-$2SiO_2$, and K_2O-$2SiO_2$. Among the interfacial systems, CN_{int} values of two, three, four, and five were observed, the most frequently observed value was one. The values were significantly lower at four and five for K_2O-$2SiO_2$ and Na_2O-$2SiO_2$, respectively. Our MD results demonstrated that the cation (Li, Na, and K)–anion environments were not the same in the interfacial domain. For further evaluation, we calculated the bond strength-coordination number, as discussed in the next section.

3.4　Bond strength-coordination number of alkali–oxygen bonds

The main aim of this analysis was to determine the relationship between σ and the interfacial structure parameter CN_{int} with bonding energy. The bond strength-coordination number of the alkali (A = Li, Na, and K)–oxygen bonds was determined as follows:

$$\text{A—O} = \frac{\sum CN_{int}}{S} U_{\text{A—O}} \tag{10}$$

where $U_{\text{A—O}}$ is the bond energy between the alkali and O, which was obtained from the literature.[5] CN_{int} was explained in the previous section. S refers to the surface area of the interface. The bond strength-coordination number has been reported for chalcogenide glasses[33]. In the present work, A—O is introduced for glass-crystal interface systems. The calculated results of A—O are plotted together with the σ values in Fig. 8. A—O clearly shows a decreasing trend in the order $\text{A—O}_{Li} > \text{A—O}_{Na} > \text{A—O}_{K}$, which is similar to σ.

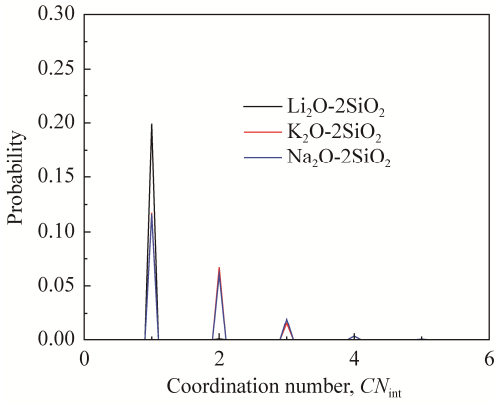

Fig. 7　Distribution of CN_{int} for various glass-crystal interfaces

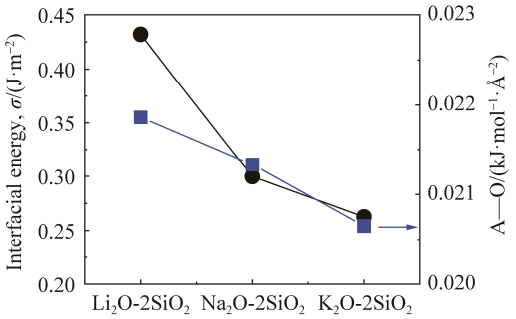

Fig. 8　Glass-crystal interfacial energy of Li_2O-$2SiO_2$, Na_2O-$2SiO_2$, and K_2O-$2SiO_2$ with the bond strength-coordination numbers for the alkali (A)–oxygen bonds (A refers to Li, Na, and K)

A relatively large difference is found between A—O_{Li} and σ_{Li}, which could be due to the potential model (see the interfacial energy section).

Thus, our proposed interface model based on MD was able to reproduce the experimental results, although the choice of potential model should be considered carefully. Analysis revealed that the alkali (Li, Na, and K)—O bond plays a crucial role in the interfacial strength. We plan to apply this model to various glass-crystal interfacial systems to obtain their interfacial energy and correlate it with nucleation rates according to classical nucleation theory, which could be useful for predicting crystal nucleation in glasses.

4 Conclusions

We developed an interface model using molecular dynamics simulations based on the minimum energy cut of crystals with glassy structures. The minimum energy cut of the crystal was determined by applying Tielemann theory. The modeled interfaces were between glass and crystals in stoichiometric alkali (Li, Na, and K) disilicates. The interface model reproduced the experimental interfacial energy trend of $\sigma_{Li} > \sigma_{Na} > \sigma_{K}$; the interatomic potential model was found to have a significant effect on reproduction. The MD results indicate that the SHIK-based MD model could reproduce the experimental results better than the other potential models.

In addition, the interfacial coordination number was also calculated, which varies depending on the alkalinity of Li, Na, and K. Using the interfacial coordination number, the bond strength-coordination number was estimated, and found that the interfacial energy trend $\sigma_{Li} > \sigma_{Na} > \sigma_{K}$ is related to the bond strength-coordination number trend of $A—O_{Li} > A—O_{Na} > A—O_{K}$.

Our proposed glass-crystal interface model can be used to estimate interfacial energies for other binary and ternary compositions, as well as to develop an approach for predicting crystal nucleation in glasses based on nucleation theory.

References:

[1] MURATA T, NAKANE S, YAMAZAKI H, et al. Heterogeneous crystal nucleation, viscosity and liquidus temperature in the system lithium metasilicate–lithium disilicate[J]. J Non Cryst Solids, 2023, 605: 122170.

[2] UEBERRICKE L, MURATA T, IKEDA H, et al. Crystal growth in oxide melts: From CALPHAD thermodynamic modeling to statistical prediction[J]. Acta Mater, 2024, 273: 119960.

[3] MAEDA E, WELCH R S, WILKINSON C J, et al. Atomistic modeling of surface nucleation in anorthite-based glasses[J]. J Non Cryst Solids, 2023, 615: 122411.

[4] FOKIN V M, ZANOTTO E D, YURITSYN N S, et al. Homogeneous crystal nucleation in silicate glasses: A 40 years perspective[J]. J Non Cryst Solids, 2006, 352(26–27): 2681–2714.

[5] TIELEMANN C, REINSCH S, MAAß R, et al. Internal nucleation tendency and crystal surface energy obtained from bond energies and crystal lattice data[J]. J Non Cryst Solids X, 2022, 14: 100093.

[6] MATUSITA K, TASHIRO M. Rate of homogeneous nucleation in alkali disilicate glasses[J]. J Non Cryst Solids, 1973, 11(5): 471–484.

[7] FOSSATI P C M, RUSHTON M J D, LEE W E. Atomic-scale description of interfaces in rutile/sodium silicate glass–crystal composites[J]. Phys Chem Chem Phys, 2018, 20(26): 17624–17636.

[8] SUN W, DIEROLF V, JAIN H. Effects of surface orientation and termination plane on glass-to-crystal transformation of lithium disilicate by molecular dynamics simulations[J]. Phys Status Solidi B: , 2021, 258(9): 2000427.

[9] SHARTSIS L, SPINNER S. Surface tension of molten alkali silicates[J]. J Res Natl Bur Stand, 1951, 46(5): 385.

[10] HOLZER M, WAURISCHK T, GEORGE J, et al. Silicate glass fracture surface energy calculated from crystal structure and bond-energy data[J]. J Non Cryst Solids, 2023, 622: 122679.

[11] SMITH R I, HOWIE R A, WEST A R, et al. The structure of metastable lithium disilicate, $Li_2Si_2O_5$[J]. Acta Crystallogr C Cryst Struct Commun, 1990, 46(3): 363–365.

[12] PANT A K, CRUICKSHANK D W J. The crystal structure of α-$Na_2Si_2O_5$[J]. Acta Crystallogr B Struct Crystallogr Cryst Chem, 1968, 24(1): 13–19.

[13] DE JONG B H W S, SUPÈR H T J, SPEK A L, et al. Mixed alkali systems: Structure and ^{29}Si MASNMR of $Li_2Si_2O_5$ and $K_2Si_2O_5$[J]. Acta Crystallogr B Struct Sci, 1998, 54(5): 568–577.

[14] PEDONE A, MALAVASI G, MENZIANI M C, et al. A new self-consistent empirical interatomic potential model for oxides, silicates, and silica-based glasses[J]. J Phys Chem B, 2006, 110(24): 11780–11795.

[15] DENG L, DU J C. Development of boron oxide potentials for computer simulations of multicomponent oxide glasses[J]. J Am Ceram Soc, 2019, 102(5): 2482–2505.

[16] SUNDARARAMAN S, HUANG L P, ISPAS S, et al. New interaction potentials for borate glasses with mixed network formers[J]. J Chem Phys, 2020, 152(10): 104501.

[17] WOLF D, KEBLINSKI P, PHILLPOT S R, et al. Exact method for the simulation of Coulombic systems by spherically truncated, pairwise r^{-1} summation[J]. J Chem Phys, 1999, 110(17): 8254–8282.

[18] PLIMPTON S. Fast parallel algorithms for short-range molecular dynamics[J]. J Comput Phys, 1995, 117(1): 1–19.

[19] NOSÉ S. A unified formulation of the constant temperature molecular dynamics methods[J]. J Chem Phys, 1984, 81(1): 511–519.

[20] HOOVER W. Canonical dynamics: Equilibrium phase-space distributions[J]. Phys Rev A Gen Phys, 1985, 31(3): 1695–1697.

[21] HOOVER W. Constant-pressure equations of motion[J]. Phys Rev A Gen Phys, 1986, 34(3): 2499–2500.

[22] BANSAL N P, DOREMUS R H. Handbook of Glass Properties[M]. Amsterdam: Elsevier, 1986.

[23] DEUBENER J, BRÜCKNER R, STERNITZKE M. Induction time analysis of nucleation and crystal growth in di- and metasilicate glasses[J]. J Non Cryst Solids, 1993, 163(1): 1–12.

[24] ZANOTTO E D. Glass crystallization research: A 36-year retrospective. Part I, fundamental studies[J]. Int J Appl Glass Sci, 2013, 4(2): 105–116.

[25] DAY D E. Mixed alkali glasses: Their properties and uses[J]. J Non Cryst Solids, 1976, 21(3): 343–372.

[26] KAWAGUCHI M, UNO M. Phase-field model for crystallization in alkali disilicate glasses: $Li_2O–2SiO_2$, $Na_2O–2SiO_2$ and $K_2O–2SiO_2$[J]. J Ceram Soc Japan, 2020, 128(10): 832–838.

[27] ZHANG Z, ISPAS S, KOB W. The critical role of the interaction potential and simulation protocol for the structural and mechanical properties of sodosilicate glasses[J]. J Non Cryst Solids, 2020, 532: 119895.

[28] HUNG S W, KIKUGAWA G, SHIOMI J. Mechanism of temperature dependent thermal transport across the interface between self-assembled monolayer and water[J]. J Phys Chem C, 2016, 120(47): 26678–26685.

[29] SAHA L C, KIKUGAWA G. Heat conduction performance over a poly(ethylene glycol) self-assembled monolayer/water interface: A molecular dynamics study[J]. J Phys Chem B, 2021, 125(7): 1896–1905.

[30] ZHAO J, GASKELL P H, CLUCKIE M M, et al. A neutron diffraction, isotopic substitution study of the structure of $Li_2O{\cdot}2SiO_2$ glass[J]. J Non Cryst Solids, 1998, 232–234: 721–727.

[31] HANNON A C, VAISHNAV S, ALDERMAN O L G, et al. The structure of sodium silicate glass from neutron diffraction and modeling of oxygen-oxygen correlations[J]. J Am Ceram Soc, 2021, 104(12): 6155–6171.

[32] PRADO R J, TIECHER F, HASPARYK N P, et al. Structural characterization of alkali-silica reaction gel: An X-ray absorption fine structure study[J]. Cem Concr Res, 2019, 123: 105774.

[33] IKEDA M, ANIYA M. Estimations and implications of the mean binding energy and the fluctuation between the structural units in chalcogenide glasses[J]. J Non Cryst Solids, 2012, 358(17): 2369–2372.

作者贡献声明：

LETON Chandra Saha：审阅与修订，初稿撰写，软件使用，模拟，验证，绘制图表，调研、分析、编程、数据整理以及论文构思；

TETSUYA Murata：审阅与修订，监督指导，项目管理以及论文构思；

SHINGO Nakane：审阅与修订，监督指导，提供资源，项目管理以及论文构思。

Molecular Dynamics Studies of Interfacial Energy in Stochiometric Alkali Disilicate Glass-Crystals Based on Crystal Minimum Energy Cutting

LETON Chandra Saha, *TETSUYA Murata*, *SHINGO Nakane*
(Fundamental Technology Division, Nippon Electric Glass, Otsu 520-8639, Shiga, Japan)

Extended Abstract

Introduction Crystallization control is crucial during glass production. In glass crystallization theory, it has been hypothesized that there is a direct relationship between glass-crystal interfacial energy and nucleation rate. Since it is difficult to measure interfacial energy directly, classical nucleation theory is used to obtain it. However, the estimation process is complex; various measurement data such as the nucleation rate, viscosity, and Gibbs free energy barriers between the glass and crystal are required. Overall, estimating the glass-crystal interfacial energy is time-consuming. In this regard, the interfacial energy can be directly obtained using molecular dynamics (MD) simulations. In this study, we implemented an interface model to estimate the glass-crystal interfacial energy based on the theory of Tielemann *et al.*, which was recently introduced to generate crystal orientation planes using minimum-energy cuts. To the best of our knowledge, this is the first work in which the crystal orientation plane determined based on a minimum-energy cutting process has been used to build a glass-crystal interface in a more realistic environment (*i.e.*, hypothesizes that a minimum-energy structure may occur during crystal nucleation) and calculate the interfacial energy. To achieve this, we considered stoichiometric alkali (Li, Na, and K) disilicate ($2SiO_2$) glasses and crystals, as some early-stage experimental data have been reported, which are highly beneficial for validating the MD results. The effects of different potential models were also investigated and found that they had a significant impact on the reproduction of the experimental trend.

Methods Simulations were performed using the LAMMPS package. The temperature and pressure were controlled with the Nose–Hoover thermostat and barostat, respectively. After setting up the glass–crystal interface using NPT, we ran MD simulations with NVT for another 200 ps to calculate the interfacial energy. The MD simulations were performed with a time step of 1 fs. Periodic boundary conditions were applied in all directions. Cutoff distances were applied according to references. We used three interatomic potential (SHIK, Du, and Pedone) models to estimate the interfacial energies of Li_2O-$2SiO_2$ glass–Li_2O-$2SiO_2$ (001), Na_2O-$2SiO_2$ glass–Na_2O-$2SiO_2$ (010), and K_2O-$2SiO_2$ glass–K_2O-$2SiO_2$ (001). All three of these potential functions are widely used. The glass structure was fabricated from the crystal structures by simulating a melt-quenching process. First, the Li_2O-$2SiO_2$ (001), Na_2O-$2SiO_2$ (010), and K_2O-$2SiO_2$ (001) crystal structures were prepared. Half the crystal was kept fixed, while the other half was melted at 3500 K with a canonical ensemble (NVT) for 300 ps and then quenched to 300 K at a cooling rate of 5 K/ps. After the melt-quenching process, the crystal part was unfixed and relaxed for 200 ps with a glassy structure using an isobaric–isothermal ensemble (NPT) at a temperature of 300 K. An interfacial model was developed by the theory of Tielemann *et al*, where the crystal plane was determined through the minimum energy cut in the crystal structure.

Results and discussion We first evaluated the glass density by calculating the local density profile along the *z*-direction of Li_2O-$2SiO_2$ glass–Li_2O-$2SiO_2$ (001), Na_2O-$2SiO_2$ glass–Na_2O-$2SiO_2$ (010), and K_2O-$2SiO_2$ glass–K_2O-$2SiO_2$ (001). The glass structures show density results comparable to the experimental data.

The calculated interfacial energy values using the SHIK potential show a similar experimental trend, while the Du and Pedone potentials are unable to reproduce the experimental trend. However, the potentials of Du and Pedone show better values of interfacial energy for the glass-crystal interface of Li_2O-$2SiO_2$ than the SHIK. Our MD results demonstrate that among the potential models, SHIK is a good candidate for calculating interfacial energy in terms of experimental reproduction.

We analyzed the interfacial coordination number (*i.e.*, cation-anion) in the contact area between the glass and crystal surfaces.

These coordination numbers are difficult to estimate experimentally. Typically, the coordination number is determined in the bulk region of a glass or crystal structure. We found that the interfacial coordination number varies significantly at the glass-crystal interface of Li_2O-$2SiO_2$, Na_2O-$2SiO_2$, and K_2O-$2SiO_2$. Among the interfacial systems, coordination number values of two, three, four, and five were observed, the most frequently observed value was one. The values were significantly lower at four and five for K_2O-$2SiO_2$ and Na_2O-$2SiO_2$, respectively. Our MD results demonstrated that the cation (Li, Na, and K)–anion environments were not the same in the interfacial domain. For further evaluation, we calculated the bond strength-coordination number.

The bond strength-coordination number has been reported for chalcogenide glasses. In the present work, the bond strength-coordination number is introduced for glass-crystal interface systems. The calculated results of bond strength-coordination number show a decreasing trend in the order Li > Na > K, which is similar to interfacial energy. Overall, analysis revealed that the alkali (Li, Na, and K)—O bond plays a crucial role in the interfacial strength.

Conclusion We developed an interface model using molecular dynamics simulations based on the minimum energy cut of crystals with glassy structures. The minimum energy cut of the crystal was determined by applying Tielemann theory. The modeled interfaces were between glass and crystals in stoichiometric alkali (Li, Na, and K) disilicates. The interface model reproduced the experimental interfacial energy trend of Li > Na > K; the interatomic potential model was found to have a significant effect on reproduction. The MD results indicate that the SHIK-based MD model could reproduce the experimental results better than the other potential models. In addition, the interfacial coordination number was also calculated, which varies depending on the alkalinity of Li, Na, and K. Using the interfacial coordination number, the bond strength-coordination number was estimated, and found that the interfacial energy trend Li > Na > K is related to the bond strength-coordination number.

Keywords glass-crystal interfacial energy; molecular dynamics simulation; interatomic potentials; interfacial coordination number